Supplementary figures for "*Metamorphic conditions of the Mesoarchean Amikoq Layered Complex, SW Greenland*"

Contents

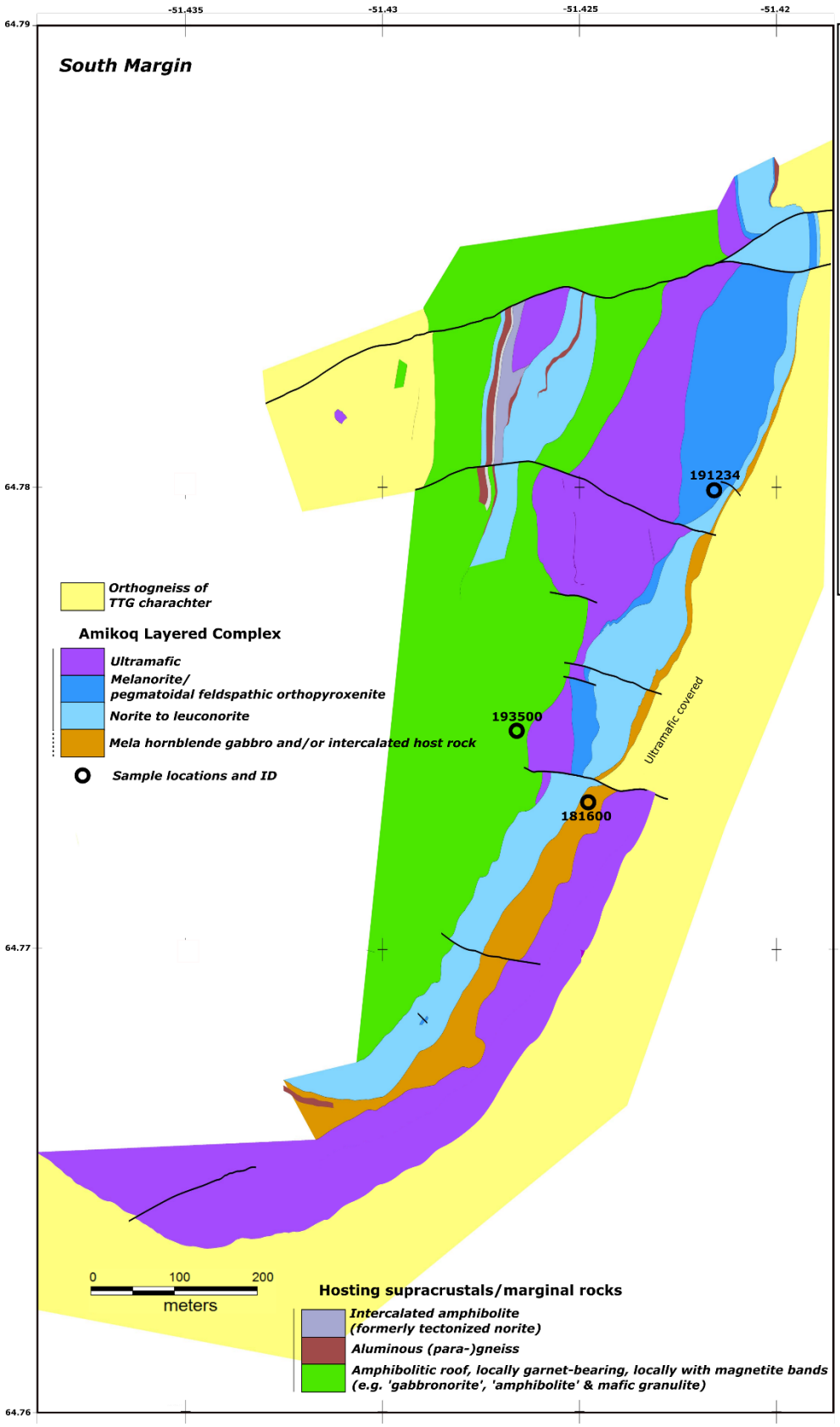

Fig. S1. Supplementary simplified geological map of South Margin. Drill cores have revealed that grey orthogneiss at the ALC-TTG boundary of South Margin contains amphibolite lenses but apparently no norite inclusions and consist of a 'gneiss/amphibolite mix' a few meters up to the norite contact (Armitage, 2010) suggesting that the majority of the ALC survived TTG intrusion. For South Margin, the "para"-prefix need to be re-evaluated in future studies owing to the close association with ultramafics (e.g. Yakymchuk & Szilas, 2018).

Fig. S1. Geological map of South Margin

Fig. S2. Additional Field photos

Fig. S2. Supplementary field photos. **a)** Finer-grained opx seem not to contain intercumulus amp while areas with coarser opx contain interstitial amp. **b)** Exposure with coarse opx and abundant intercumulus amp. **c)** Field relations at South Margin, with intercalated mela-amphibolite in the foreground, overlain by norite and pegmatoidal orthopyroxenites/melanorites. See Fig. S1. **d)** Example of extreme garnet norite at West Margin with a transition across strike from 'pure' leuconorite into the garnetiferous zone and out again. **e)** Garnet norite from South Margin. **f)** Aluminous gneiss with large garnet porphyroblasts.

Fig. S3. Zircon image and $^{207}Pb/^{206}Pb$ vs. $^{238}U/^{206}Pb$

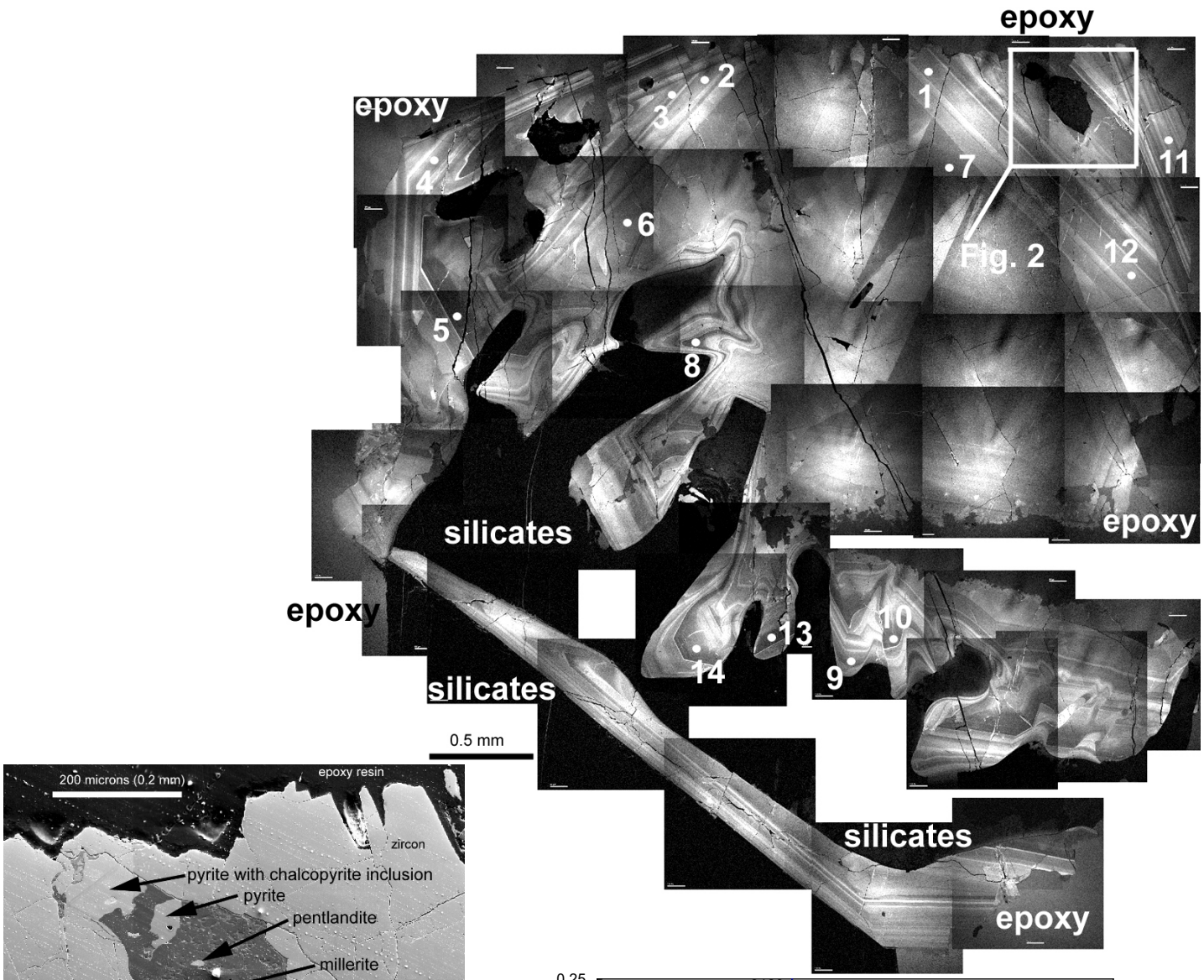

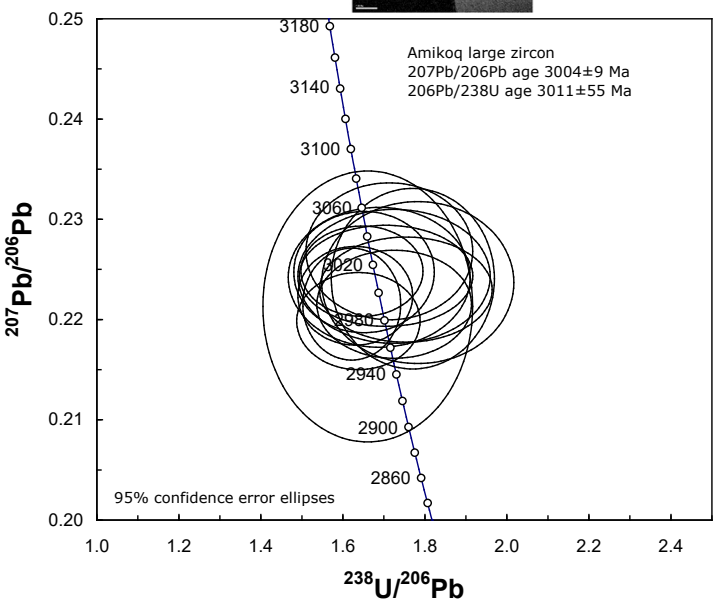

Fig. S3. SHRIMP U-Pb dated Amikoq zircon mega-cryst. **a)** Cathodoluminescence (CL) image mosaic on polished, sectioned zircon from drill hole FF-DDH-06-39 (188.68 m). Numbered spots are the sites of SHRIMP U-Pb analysis, shown at their true size. **b)** Back Scattered Electron image of inclusion in zircon (see Fig. S3a for location). The NW-SE 'grain' across the image is slight damage to the gold coat, and is not part of the sample. **c)** $^{238}U/^{206}Pb$ versus $^{207}Pb/^{206}Pb$ plot for Amikoq zircon analyses.

Fig. S4. Additional thin section photos (Sil-grt-crd gneiss) (500 dpi)

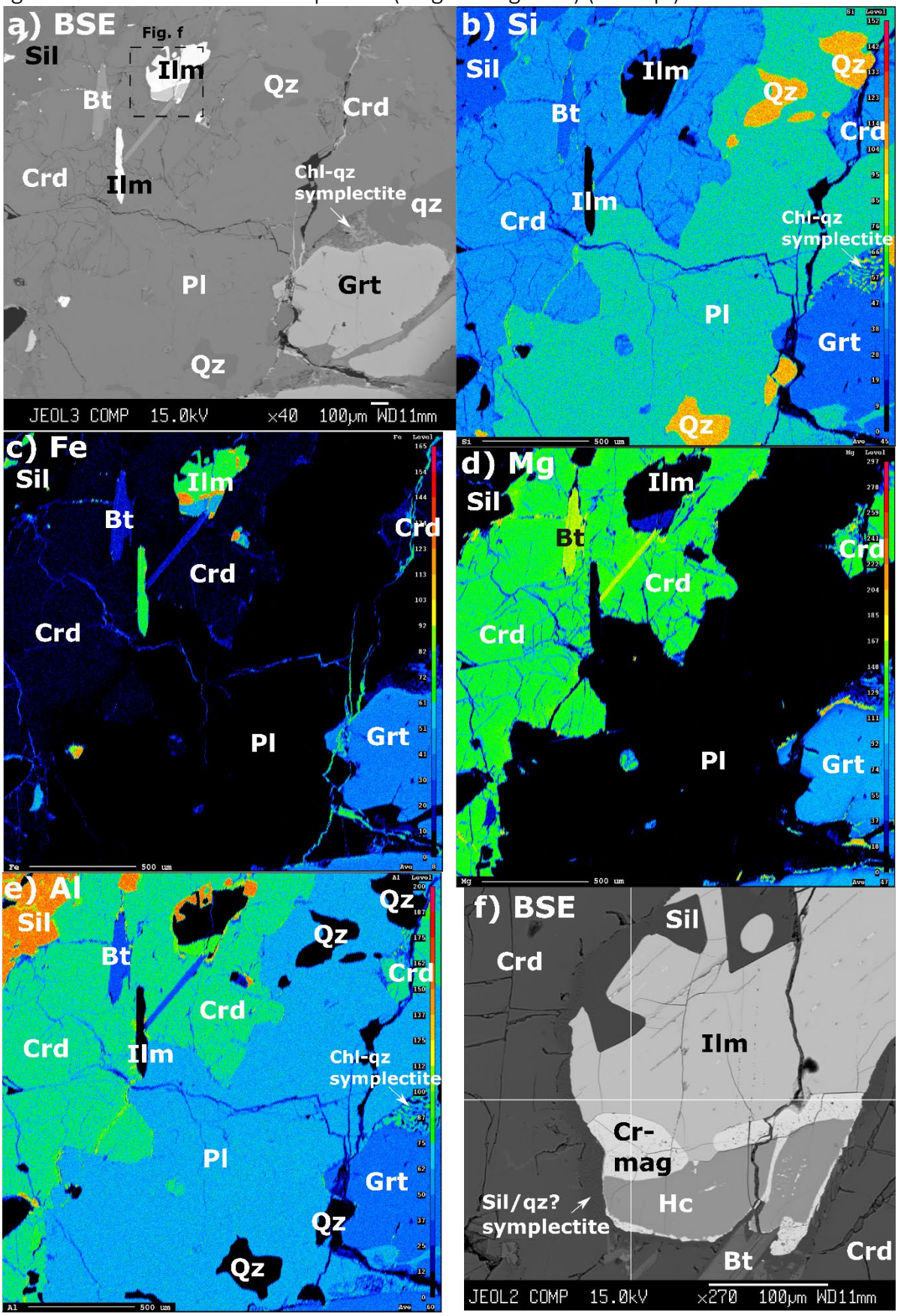

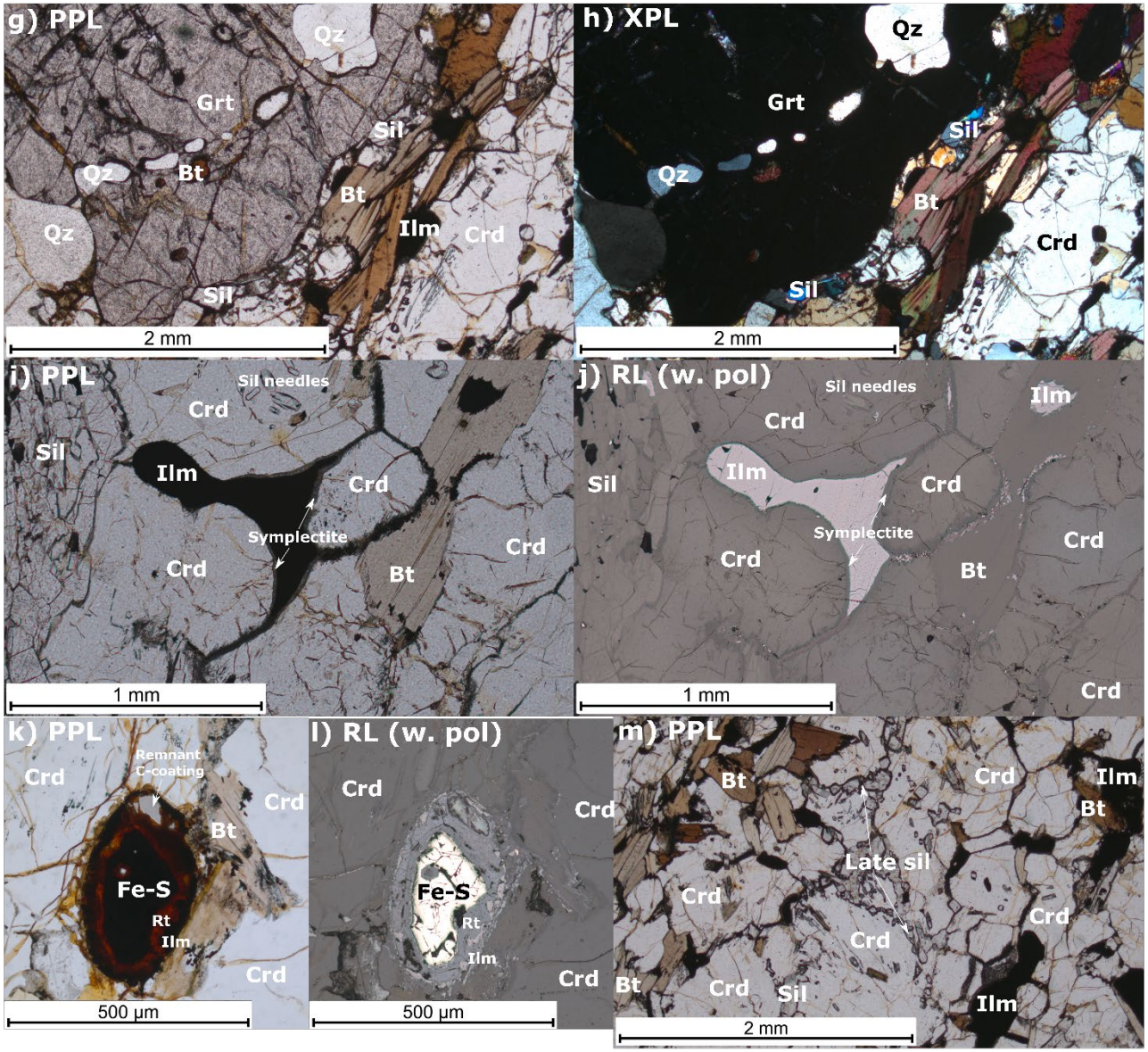

Fig. S4. Supplementary photos and compositional maps of the marginal sil-grt-crd paragneiss (191142). **a)** Image illustrating the general mineralogy, coronitic pl + qz on grt, chl + qz symplectite breakdown of grt and composite oxide grain with partial replacement by sil. Upper left corner is a small part of a bifurcating sil + ilm nematoblastic band. Part of the blue grt in Fig. S16. BSE. **b)** Si-intensity map of a). **c)** Fe-intensity map of a). **d)** Mg-intensity map of a). **e)** Al-intensity map of a). **f)** Zoom-in of composite oxide, see a). The Cr-mag is probably formed through Al-leaching by sil. BSE. **g)** Part of the blue grt in Fig. S16. The grt contain blebs of qz and bt-grains, with a rim bounded by sil + bt + ilm ± crd ± qz. The rim sil + bt + ilm is likely later than the peak grt core + crd assemblage. PPL. **h)** XPL of g). **i)** Decomposition of crd and bt forming new ilm at former crd grain boundaries. Note sil band on the left side, with near-vertical orientation while small sil-needles in crd have a more horizontal orientation. PPL **j)** RL with polarizer in, of i). **k)** Small composite grain with concentrical layering that possibly reflect changing P-T conditions preserved through continuous armouring. A type of Fe-sulfide, likely pyrite form the centre, with a middle layer of rt (judging from colours in PPL), finally overgrown by a thin ilm layer. Both Fe-sulfide and a small rt grain have been found in a grt-core. PPL. **l)** Same as k) but in RL with polarizer in. **m)** Image illustrating the growth of late granular sil at crd grain boundaries, as well as bt and ilm. PPL. Chemical map parameters: 1024x1024 pixels, 2µm pixel size, 60 msec dwell time. *Abbreviations:* Grt = garnet, Bt = biotite, Sil = sillimanite, Crd = cordierite, Spl = Spinel, Cr-mag = Cr-magnetite (ferritchromite), Hc = Hercynite, Ilm = ilmenite, Chl = chlorite, Pl = plagioclase, Qz = quartz, Rt = Rutile, PPL = plane polarized light, XPL = extra polarized light, BSE = Back-scattered electron, RL = Reflected light.

Fig. S5. Additional thin section photos (K-hastingsite gneiss) (part 1: 500 dpi)

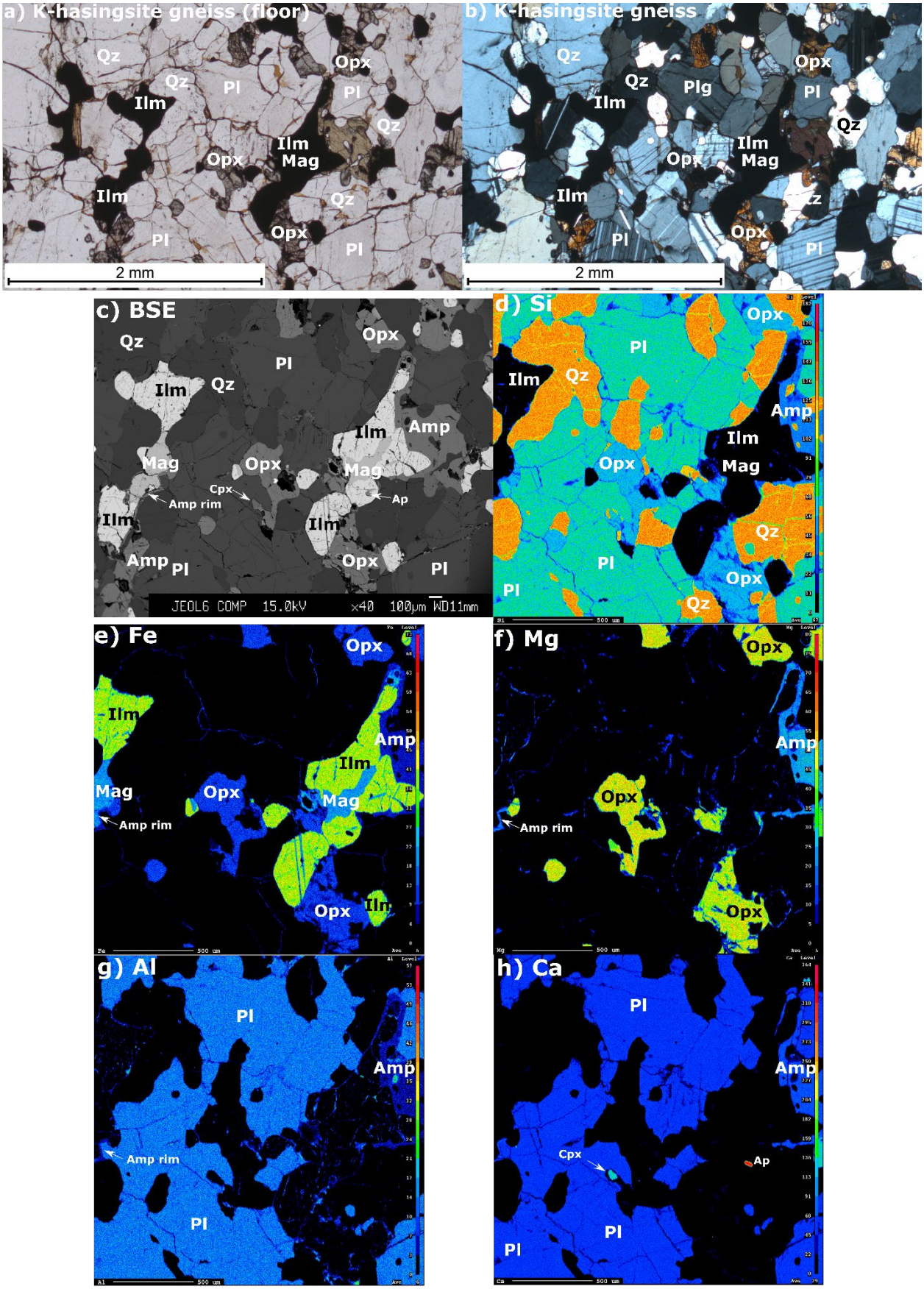

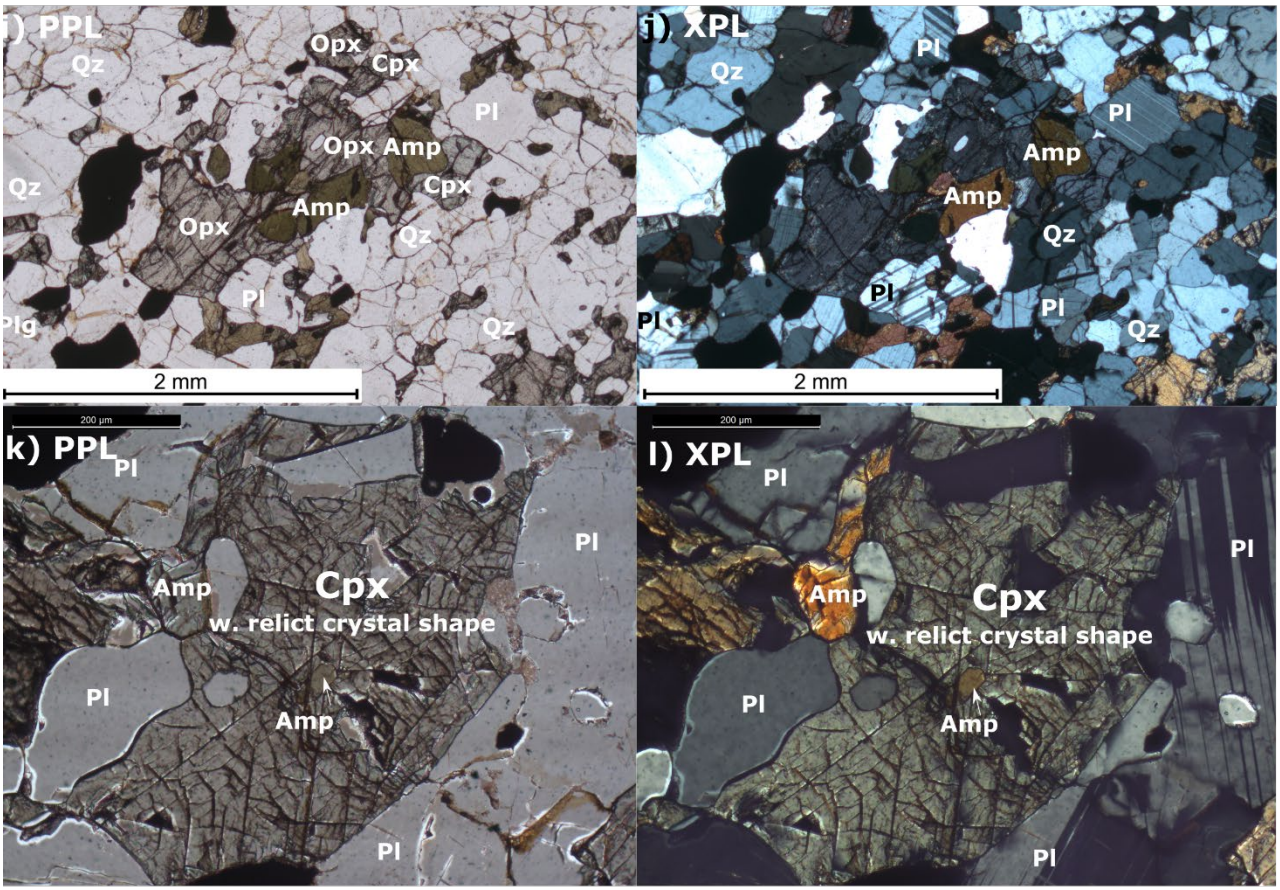

Fig. S5. Supplementary photos and compositional maps of the marginal K-hastingsite gneiss of supracrustal 'amphibolitic' affinity (191143). **a)** Image illustrating the general mineralogy. Amphibole tend to grow on oxides and pyroxenes. PPL. **b)** XPL of a). **c)** BSE of a). Ilm and mag are well exsolved, showing "granular" intergrain relation; see Fig. 9 of the main text. BSE. **d)** Si-intensity map of c). **e)** Fe-intensity map of c). **f)** Mg-intensity map of a). **g)** Al-intensity map of c). **h)** Ca-intensity map of c). **i)** Pyroxene and amp intergrowth. PPL. **j)** XPL of g). **k)** Large cpx grain with relict crystal shape. PPL **l)** XPL of k). Chemical map parameters: 1024x1024 pixels, 2µm pixel size, 20 msec dwell time. *Abbreviations:* Opx = orthopyroxene, Cpx = clinopyroxene, Amp = Amphibole, Ap = apatite, Mag = magnetite, Ilm = ilmenite, Pl = plagioclase, Qz = quartz, PPL = plane polarized light, XPL = extra polarized light, BSE = Back-scattered electron.

Fig. S6. Additional thin section photos (Mafic granulite)

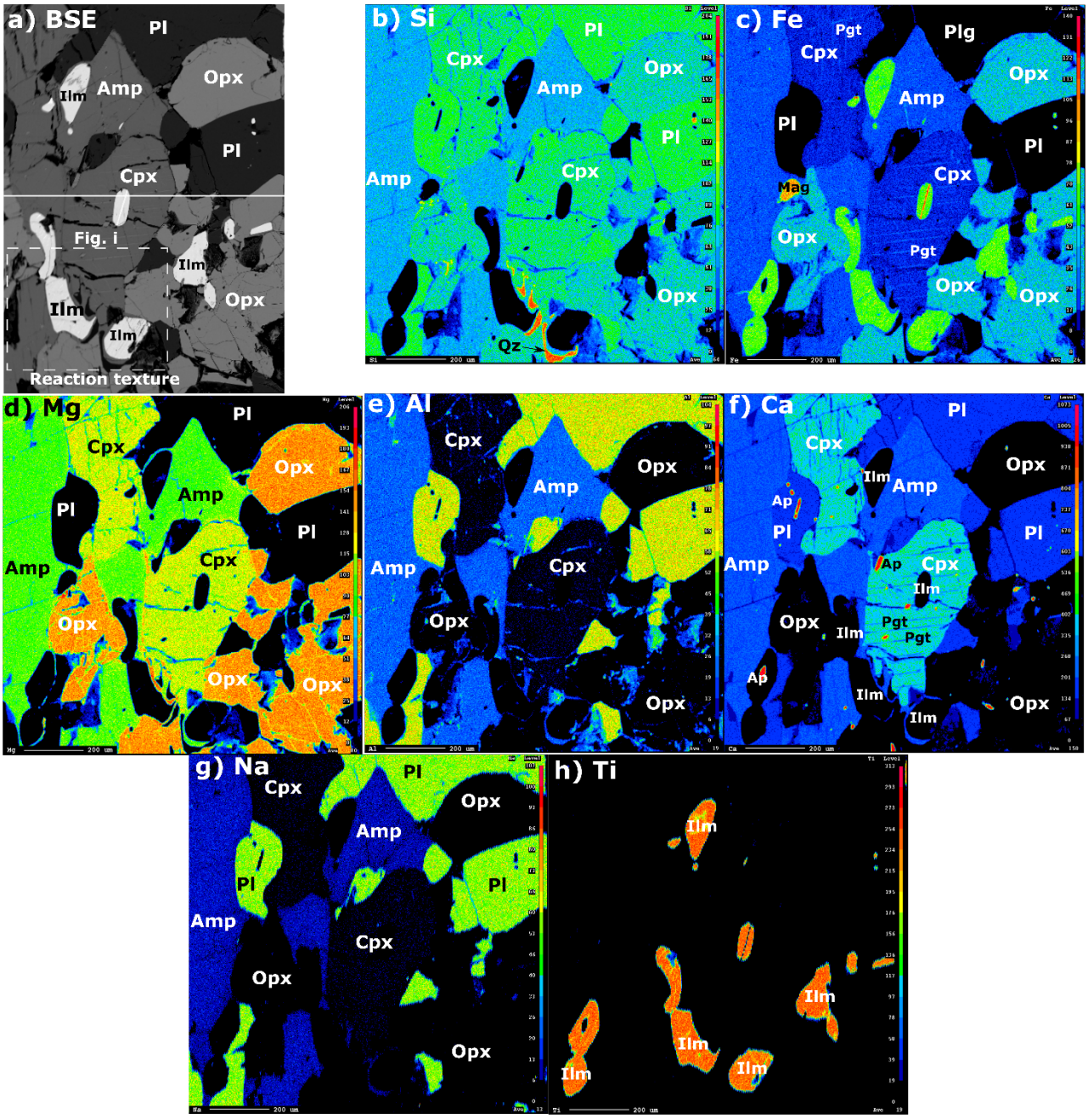

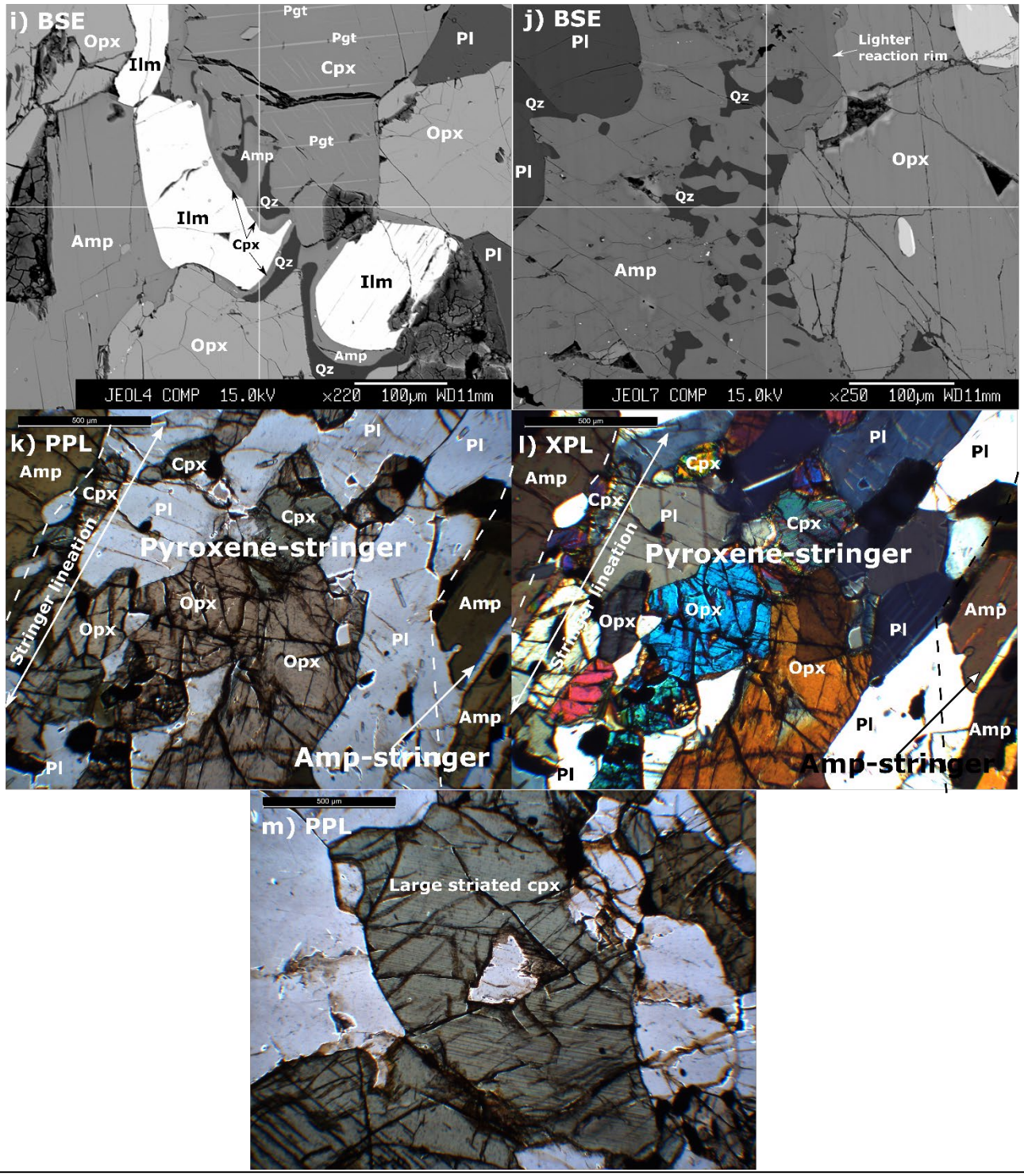

Fig. S6. Supplementary photos and compositional maps of supracrustal roof 'amphibolitic' mafic granulite (sample 193500). **a)** Zoom-in of Fig. 4b in the main text, illustrating the general mineralogy. Amphibole show pseudomorphic replacement of cpx, with a core of relict cpx that contain pgt exsolution lamellae. BSE. **b)** Si-intensity map of a). **c)** Fe-intensity map of a). **d)** Mg-intensity map of a). **e)** Al-intensity map of a). **f)** Ca-intensity map of a). **g)** Na-intensity map of a). **h)** Ti-intensity map of a). **i)** Zoom-in of the reaction in a). The analysed "cpx" of this zone has major element characteristics typical both of cpx and amp (Table S5), implying it is a hybrid and locks in the transition from amp + qz = cpx; since qz is not common in the thin section, the reaction is inferred to be of retrogressive origin – see main text for more details. BSE. **j)** Breakdown reaction of opx to amp + qz. BSE. **k)** Stringer-fabric, illustrated here with a pyroxene-dominated stringer flanked by amp-dominated stringers. PPL **l)** XPL of i). **m)** Tiger-striped cpx grain, where the "stripes" are pgt exsolution lamellae. PPL. Chemical map parameters: 600x600 pixels, 2µm pixel size, 60 msec dwell time. *Abbreviations:* Opx = orthopyroxene, Cpx = clinopyroxene, Pgt = pigeonite, Amp = Amphibole, Ap = apatite, Mag = magnetite, Ilm = ilmenite, Pl = plagioclase, Qz = quartz, PPL = plane polarized light, XPL = extra polarized light, BSE = Back-scattered electron.

Fig. S7. Additional thin section photos (dunite/harzburgite)

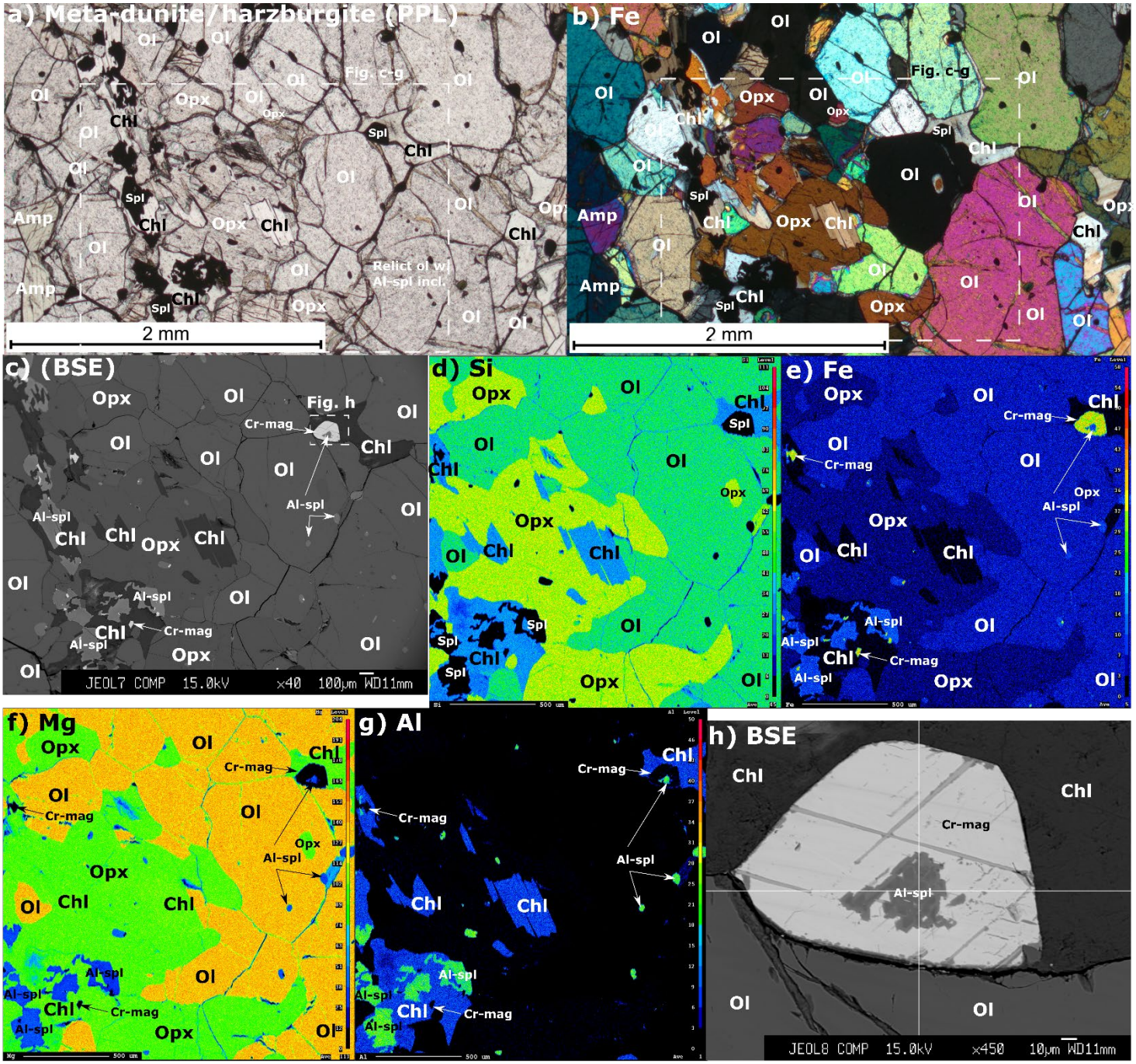

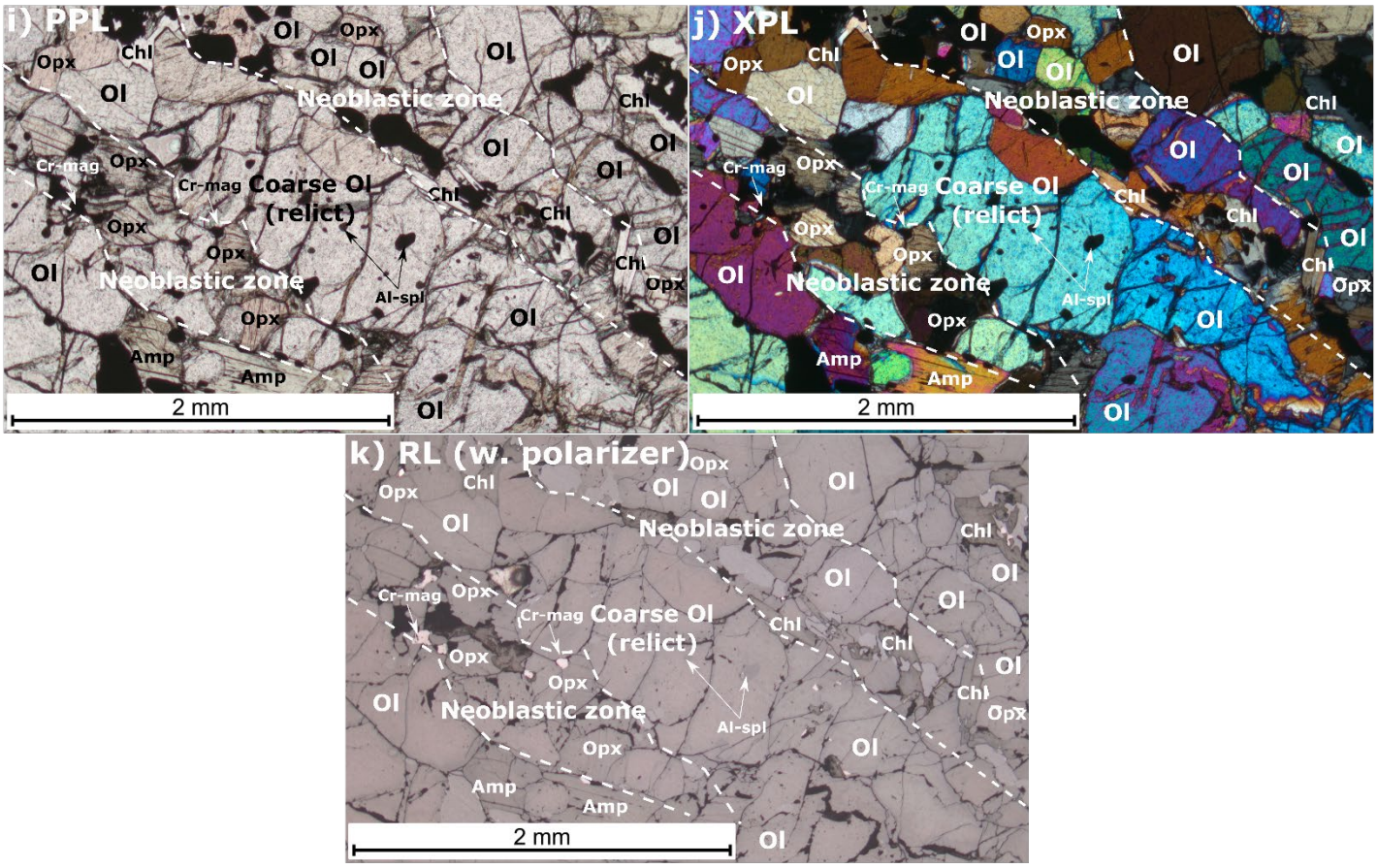

Fig. S7. Supplementary photos and compositional maps of dunite/harzburgite (191147) from a West Margin ultramafic lens. **a)** Image illustrating the general mineralogy, with emphasis on the granoblastic texture and retrograde chl + Cr-mag formation. PPL. **b)** XPL of a). **c)** BSE of area outlined in a). Note the inclusions in olivine. BSE. **d)** Si-intensity map of c). **e)** Fe-intensity map of c). **f)** Mg-intensity map of c). **g)** Al-intensity map of c). **h)** Zoom-in as indicated in c), illustrating the relict Al-spl which has been replaced by Cr-mag due to Al-leaching during chl formation. BSE. **i)** Zones of coarse Al-spl inclusion filled olivine of probable relict origin flanked by zones of largely inclusion-free neoblastic olivine. PPL. **j)** XPL of i). k**)** RL with polarizer, of i). Chemical map parameters: 1024x1024 pixels, 2µm pixel size, 20 msec dwell time. *Abbreviations:* Ol = olivine, Cr-mag = Chrome-magnetite, Al-spl = spinel (*s.s.*), Chl = chlorite, Opx = orthopyroxene, Amp = Amphibole, PPL = plane polarized light, XPL = extra polarized light, BSE = Back-scattered electron, RL = Reflected light. Note that cummingtonite lamellae occur in hornblende, consistent with equilibration with orthopyroxene.

Fig. S8. Additional thin section photos (olivine orthopyroxenite)

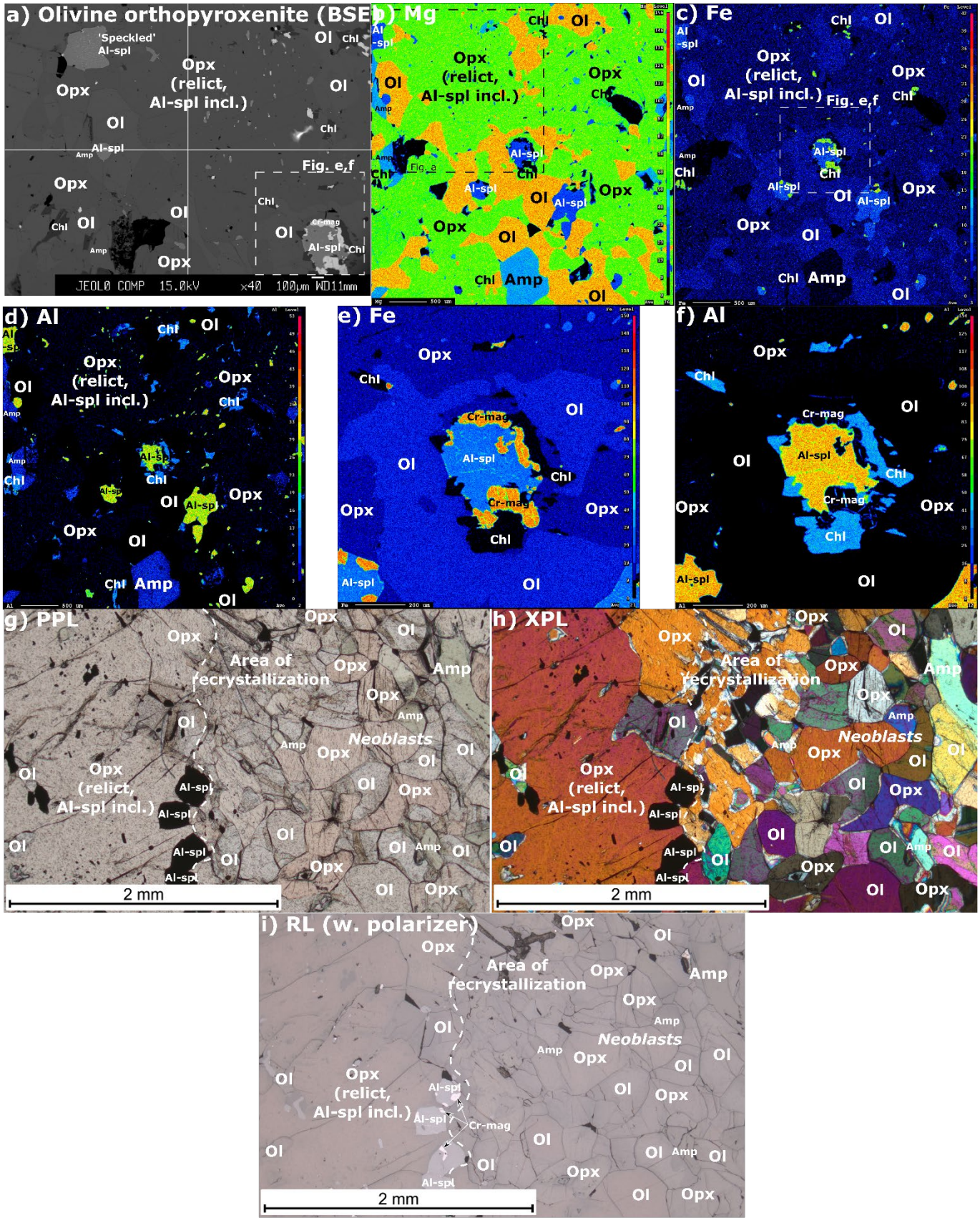

Fig. S8. Supplementary photos and compositional maps of olivine orthopyroxenite (191150, adjacent to the dunite/harzburgite in Fig. S7; see Fig. 2 of the main text for location) from a West Margin ultramafic lens. **a)** Image illustrating the general mineralogy, with emphasis on the large relict opx and retrograde chl + Cr-mag formation. BSE. **b)** Mg-intensity map overlapping a). **c)** Fe-intensity map overlapping a). **d)** Al-intensity map overlapping a). **e)** Fe-intensity map. Zoom-in on composite spinel, see a) and c) for position. Like Fig. S7f, it is illustrated how Cr-mag is coeval with chl owing to Al-leaching by chl of the original Al-spl. **f)** Al-intensity map of e). **g)** Zones of coarse Al-spl inclusion filled opx of probable relict origin flanked to the right by a zone of largely inclusion-free neoblasts. PPL. **h)** XPL of g). **i)** RL with polarizer, of g). Chemical map parameters: of b-d - 800x800 pixels, 5µm pixel size, 12 msec dwell time; of e-f – 600x600 pixels, 2µm pixel size, 60 msec dwell time. *Abbreviations:* Ol = olivine, Cr-mag = Chrome-magnetite, Al-spl = spinel (*s.s.*), Chl = chlorite, Opx = orthopyroxene, Amp = Amphibole, PPL = plane polarized light, XPL = extra polarized light, BSE = Back-scattered electron, RL = Reflected light.

Fig. S9. Additional thin section photos (Orthopyroxenite)

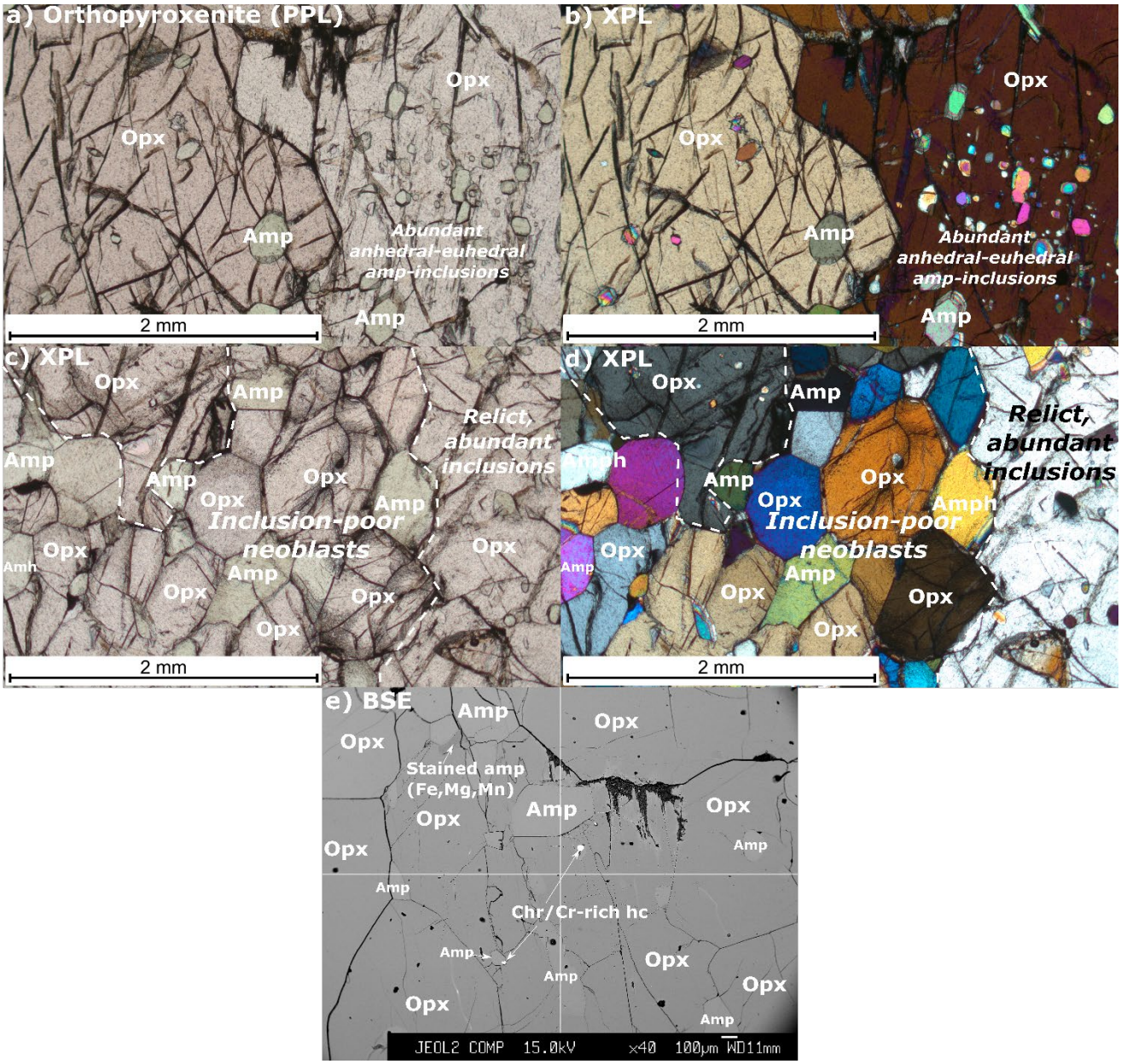

Fig. S9. Supplementary photos and BSE-image of meta-orthopyroxenite (181584, adjacent to the dunite/harzburgite and olivine orthopyroxenite in Fig. S7 & S8; see Fig. 2 of the main text) from a West Margin ultramafic lens. **a)** Image illustrating the general mineralogy, which is almost exclusively composed of large opx-grains with abundant amp-inclusions. PPL. **b)** XPL of a). **c)** Area of neoblast formation, where large relict opx grains have broken down into more equigranular, granoblastic aggregates of opx + amp. PPL **d)** XPL of c) **e)** Image displaying the very rare occurrences of chromite and Cr-rich hc. Note also beginning retrograde formation of Fe,Mg,Mn-amp. BSE. *Abbreviations:* Opx = orthopyroxene, Amp = Amphibole, Chr = chromite, Cr-rich hc = Cr-rich hercynite, PPL = plane polarized light, XPL = extra polarized light, BSE = Back-scattered electron.

Fig. S10. Additional thin section photos (Melanorite)

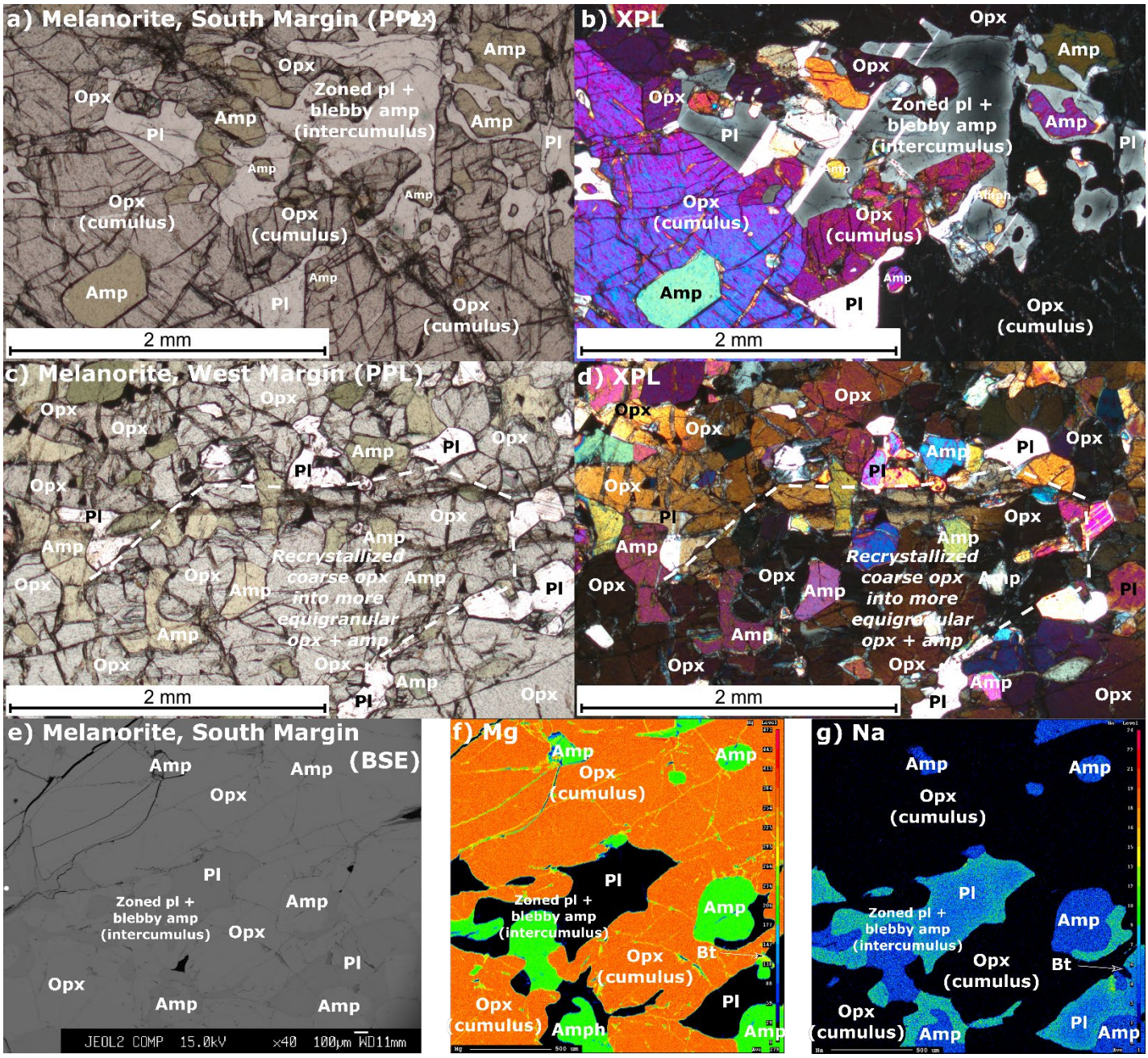

Fig. S10. Supplementary photos and compositional maps of West- and South Margin melanorites (191146 & 191234, respectively), where especially the latter have preserved igneous textures. **a)** Cumulus texture, with unaligned cumulus subhedral-euhedral opx and intercumulus amp + zoned and poikilitic pl, ocassionally intergrown in a blebby fashion. PPL **b)** XPL of a). **c)** Large opx grain, which has broken down into more equigranular opx + amp aggregate, similar to Fig. S9g-h & S10c-d. PPL. **d)** XPL of c). **e)** BSE image of the South Margin melanorite that host relict igneous textures. **f)** Mg-intensity map of e). **g)** Na-intensity map of g). Note the increasing Na-content rimwards in the plagioclase. Chemical map parameters: 1024x1024 pixels, 2µm pixel size, 60 msec dwell time. *Abbreviations:* Opx = orthopyroxene, Amp = Amphibole, Pl = plagioclase, Bt = biotite, PPL = plane polarized light, XPL = extra polarized light, BSE = Back-scattered electron.

Fig. S11. Additional thin section photos (Norite)

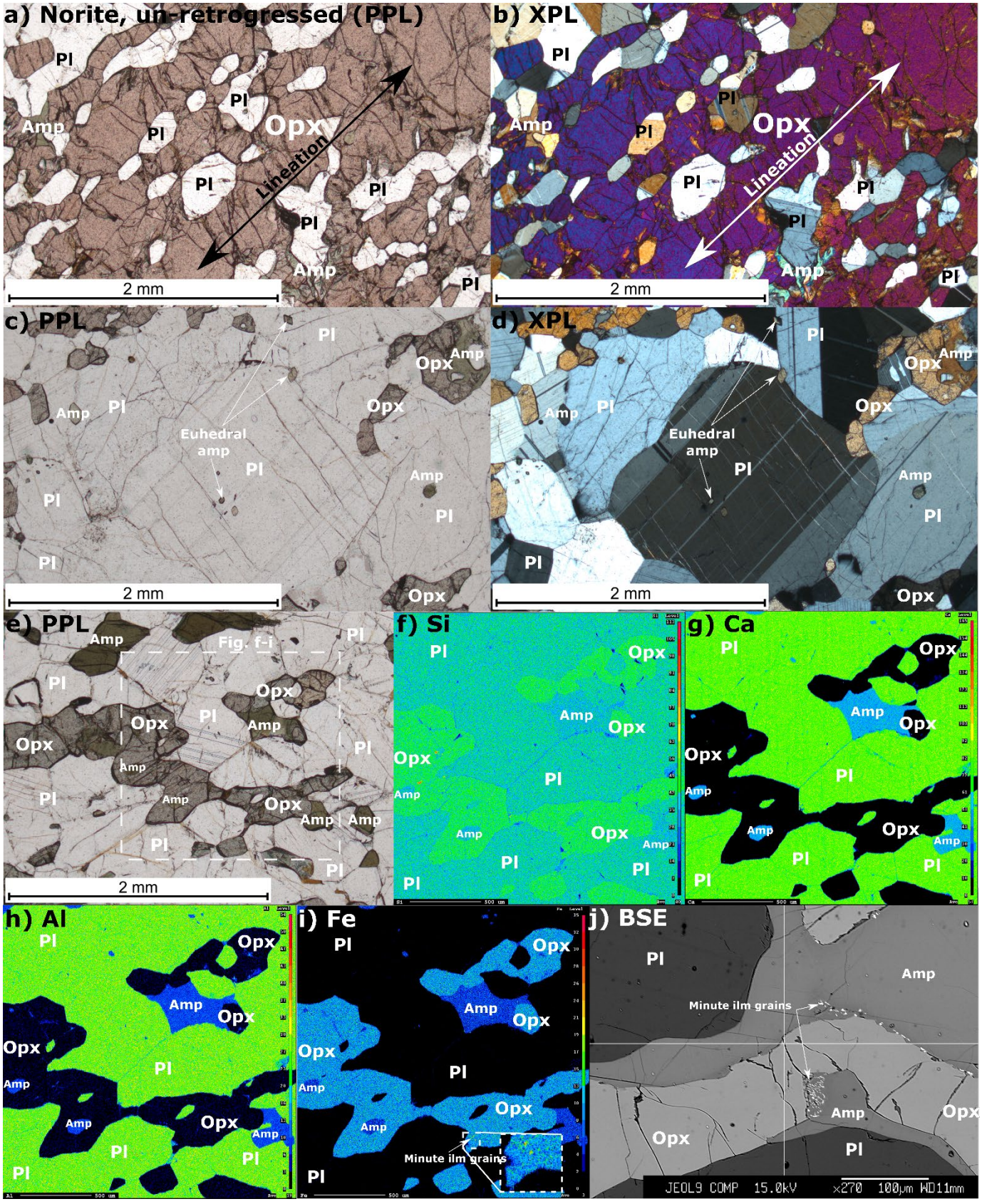

Fig. S11. Supplementary photos and compositional maps of an un-retrogressed West Margin norite (181760). **a)** Opx-dominated area, ranging to melanoritic mineral modes. Note the rarity of amp and the lineated opx-stringers, which nevertheless appear to be optically continuous. PPL **b)** XPL of a). **c)** Plagioclase-dominated area, ranging to leuconorite or anorthosite mineral modes. Note small euhderal amp inclusions. PPL. **d)** XPL of c). **e)** Typical area, with a partly replaced opx-stringer. **f)** Si-intensity map of indicated area in e). **g)** Ca-intensity map of indicated area in e). **h)** Al-intensity map of indicated area in e). **i)** Fe-intensity map of indicated area in e). **j)** Image illustrating the minute ilm-exsolution grains that occasionally occur in amp. Chemical map parameters: 1024x1024 pixels, 2µm pixel size, 60 msec dwell time. *Abbreviations:* Opx = orthopyroxene, Amp = Amphibole, Pl = plagioclase, Bt = biotite, PPL = plane polarized light, XPL = extra polarized light, BSE = Back-scattered electron.

Fig. S12. Additional thin section photos (retrogressed norite) (500 dpi)

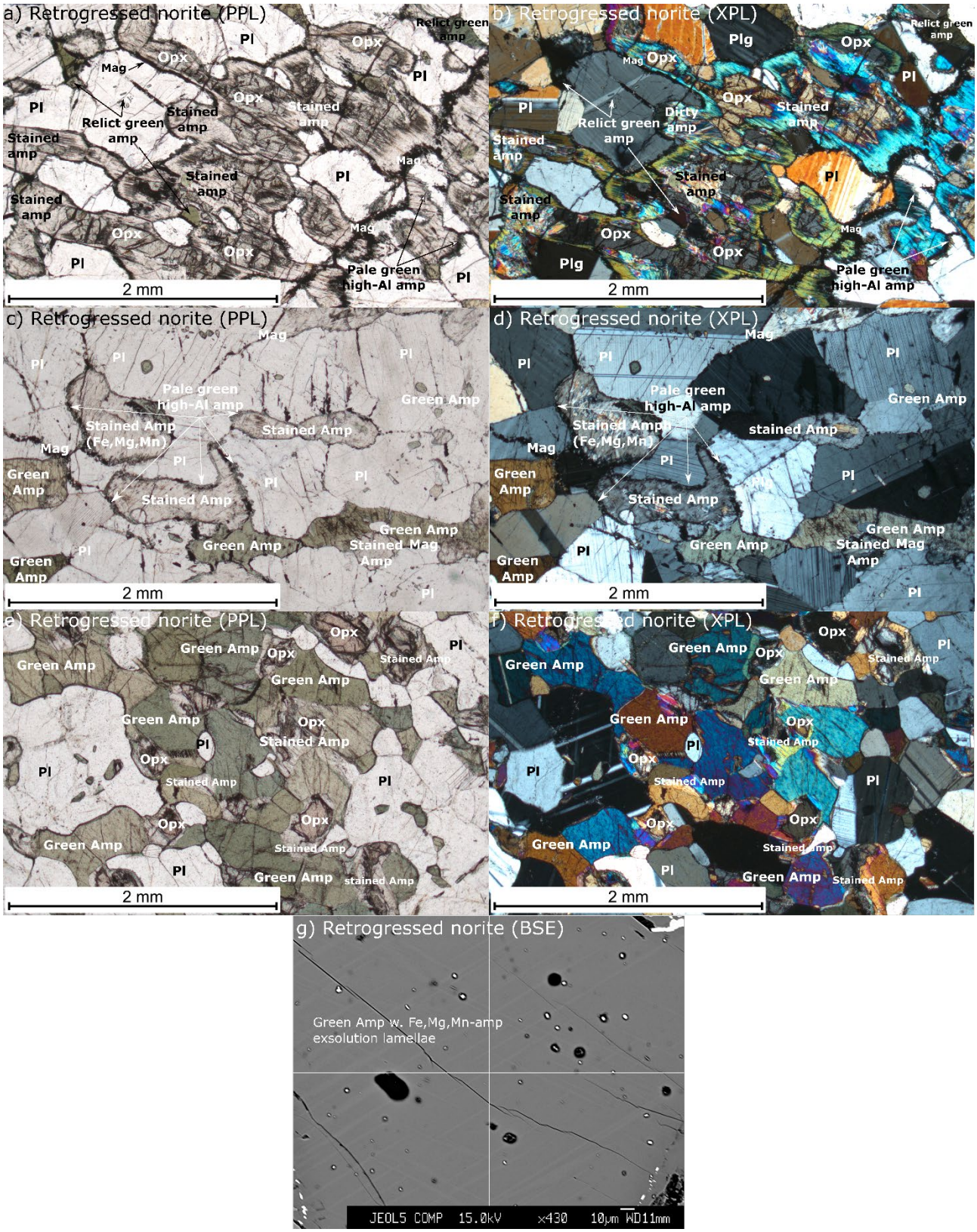

Fig. S12. Supplementary photos and compositional maps of retrogressed West Margin norites (181785 & 181791). **a)** Typical area with extensively retrogressed opx, which has been nearly completely altered to stained (Fe,Mg,Mn)-amp barring a few relict opx cores. Relict opx crystal margins are demarcated by mag. Note that green Ca-amp survived the retrogression, though their geochemistry indicate re-equilibration (see main text). For BSE image, see Fig. 4b. PPL **b)** XPL of a). **c)** Plagioclase-dominated area. Area with three co-existing amp – green Ca-amp, stained (Fe,Mg,Mn)-amp and pale green high-Al Ca-amp at pl-relict opx grain boundaries. PPL. **d)** XPL of c). **e)** Dominantly green Ca-amp with some relict opx cores and some stained (Fe,Mg,Mn)-amp replacement. **f)** XPL of e). **g)** Zoomed in BSE image of a green Ca-amp with (Fe,Mg,Mn)-amp exsolution lamellae, which probably is coeval with the opx-replacement in Fig. a-d. *Abbreviations:* Opx = orthopyroxene, Amp = Amphibole, Pl = plagioclase, Mag = magnetite, PPL = plane polarized light, XPL = extra polarized light, BSE = Back-scattered electron.

Fig. S13. Additional thin section photos (mela hornblende gabbro) (500 dpi)

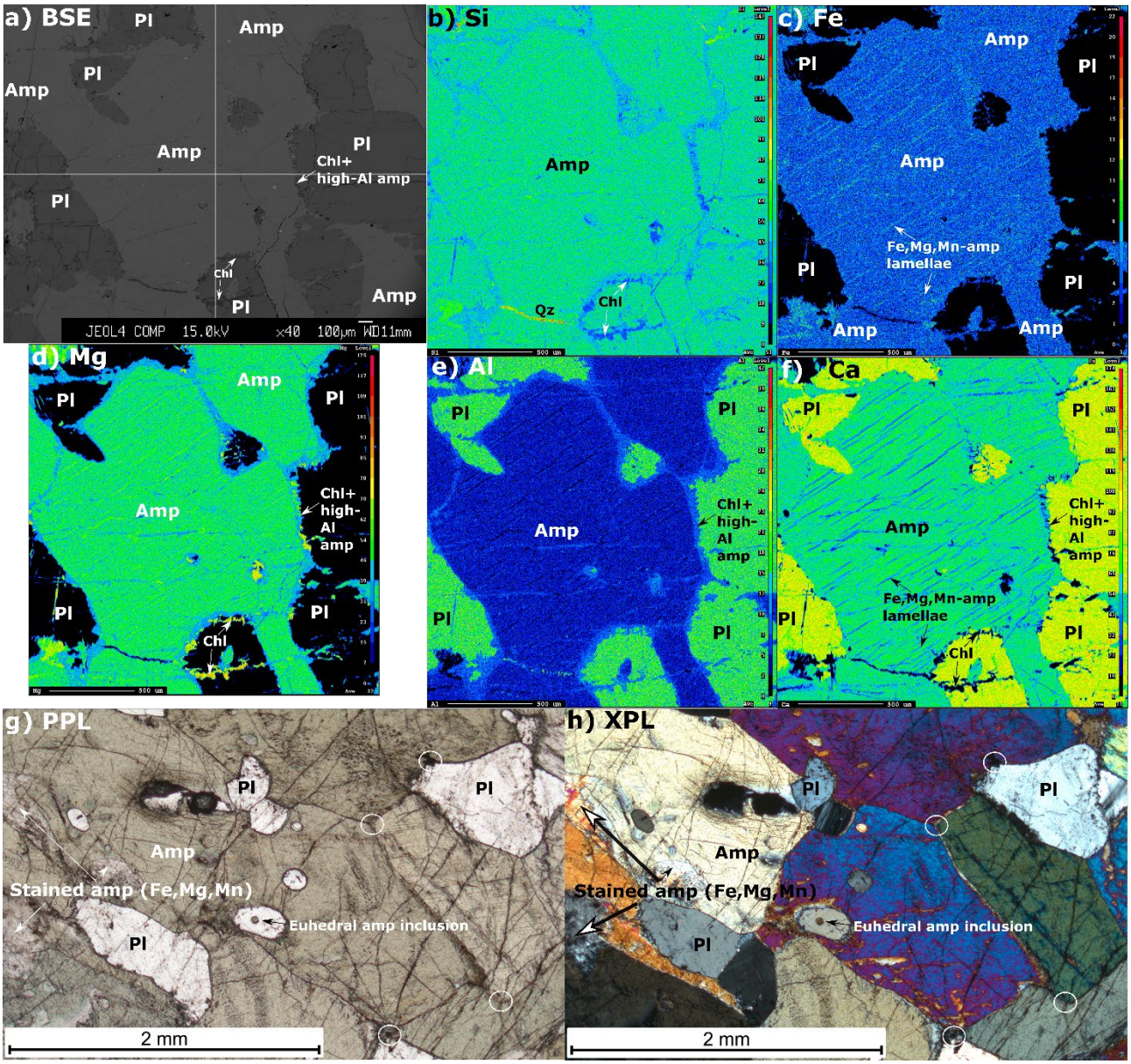

Fig. S13. Supplementary photos and compositional maps of mela-hornblende gabbro (181600). **a)** Image illustrating the general mineralogy, with emphasis on the Fe,Mg,Mn-amp exsolution lamellae in the green Ca-amp and secondary pale-green high-Al Ca-amp + chl ± qz formed at green Ca-amp and pl boundaries. BSE. **b)** Si-intensity map of a). **c)** Fe-intensity map of a). **d)** Mg-intensity map of a). **e)** Al-intensity map of a). **f)** Ca-intensity map of a). **g)** Typical part, dominated by granoblastic green Ca-amp, blebby pl and small euhedral green Ca-amp. Some areas of the green Ca-amp is retrogressed to stained Fe,Mg,Mn-amp. Circles mark mosaic junctions. PPL. **h)** XPL of g). Chemical map parameters: 1024x1024 pixels, 2µm pixel size, 20 msec dwell time. *Abbreviations:* Amp = Amphibole, Pl = plagioclase, Qz = quartz, Chl = chlorite, PPL = plane polarized light, XPL = extra polarized light, BSE = Back-scattered electron.

Fig. S14. MnO in olivine (500 dpi)

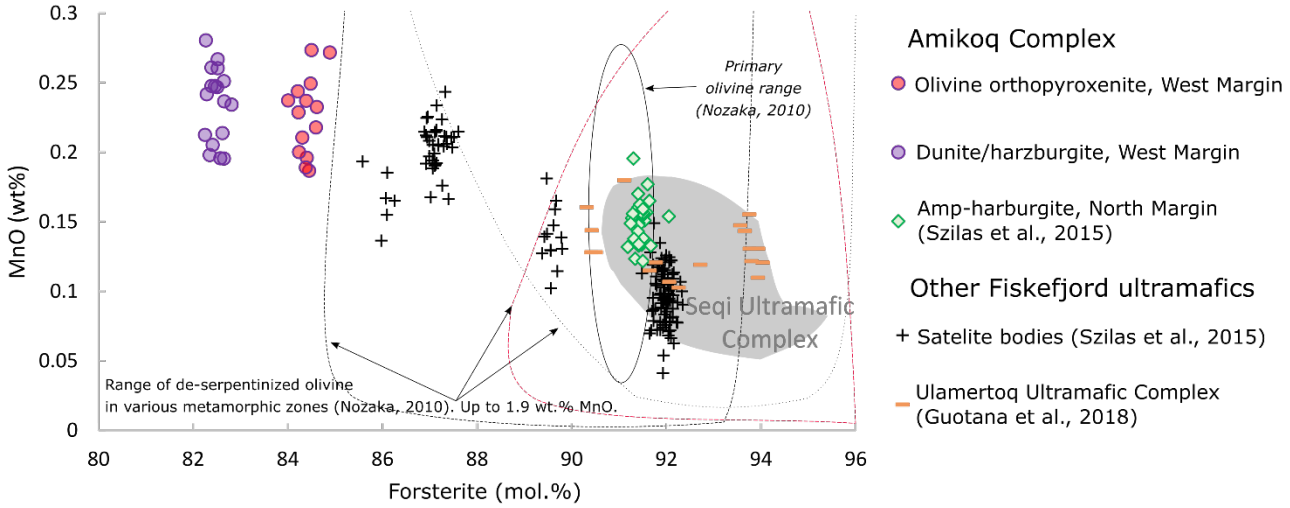

Fig. S14. Olivine of Amikoq and the Fiskefjord region. Olivine MnO (wt.%) vs. olivine forsterite content (mol.%). The range of various olivine formed through de-serpentinization have been plotted to illustrate the great range (Nozaka, 2010) relative to the narrow range observed in individual Fiskefjord olivine-occurrences, and especially Amikoq. The 'Primary olivine range' illustrate the narrow range expected from igneous olivine, consistent with Fiskefjord olivine. Red field mark the highest metamorphic grade of Nozaka (2010).

Fig. S15. Pyroxenes, according to Morimoto (1988) (500 dpi)

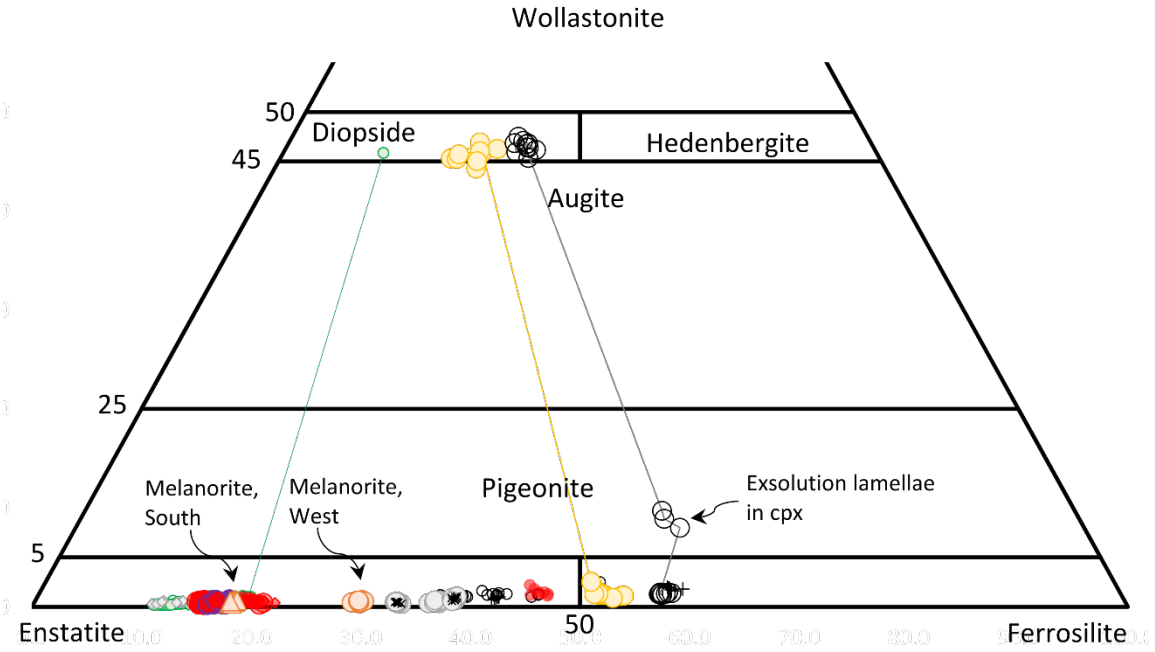

Amikoq Complex

- Dunite/harzburgite, West Margin
- Olivine orthopyroxenite, West Margin
- Orthopyroxenite, West Margin
- Melanorite, West Margin
- Norite, West Margin
- Retrogressed norite, West Margin
- Melanorite, South Margin
- Peridotite, West Margin (Kristensen, 2006)
- Pyroxenites, North Margin (Kristensen, 2006)
- Norite, North Margin (Kristensen, 2006)

Supracrustals/marginal rocks

- K-hastingsite 2-px gneiss (floor)
- Mafic granulites, amphibolites etc. (host rocks)
- 'Tectonized norites' (Kristensen, 2006), intercalated amphibolites

Fig. S15. Pyroxene quadrilateral with mineral compositions according to Morimoto (1988). Pyroxenes from Kristensen (2006) are plotted as reported and have not been recalculated except for the single clinopyroxene analysis. The low-En pyroxenite of Kristensen (2006) is probably a type of host supracrustal (see also Fig. 7 of the main text). Small symbols are from Kristensen (2006).

Fig. S16. Ca-amp diagram after Hawthorne et al., 2012 & Cr_2O_3 (500 dpi)

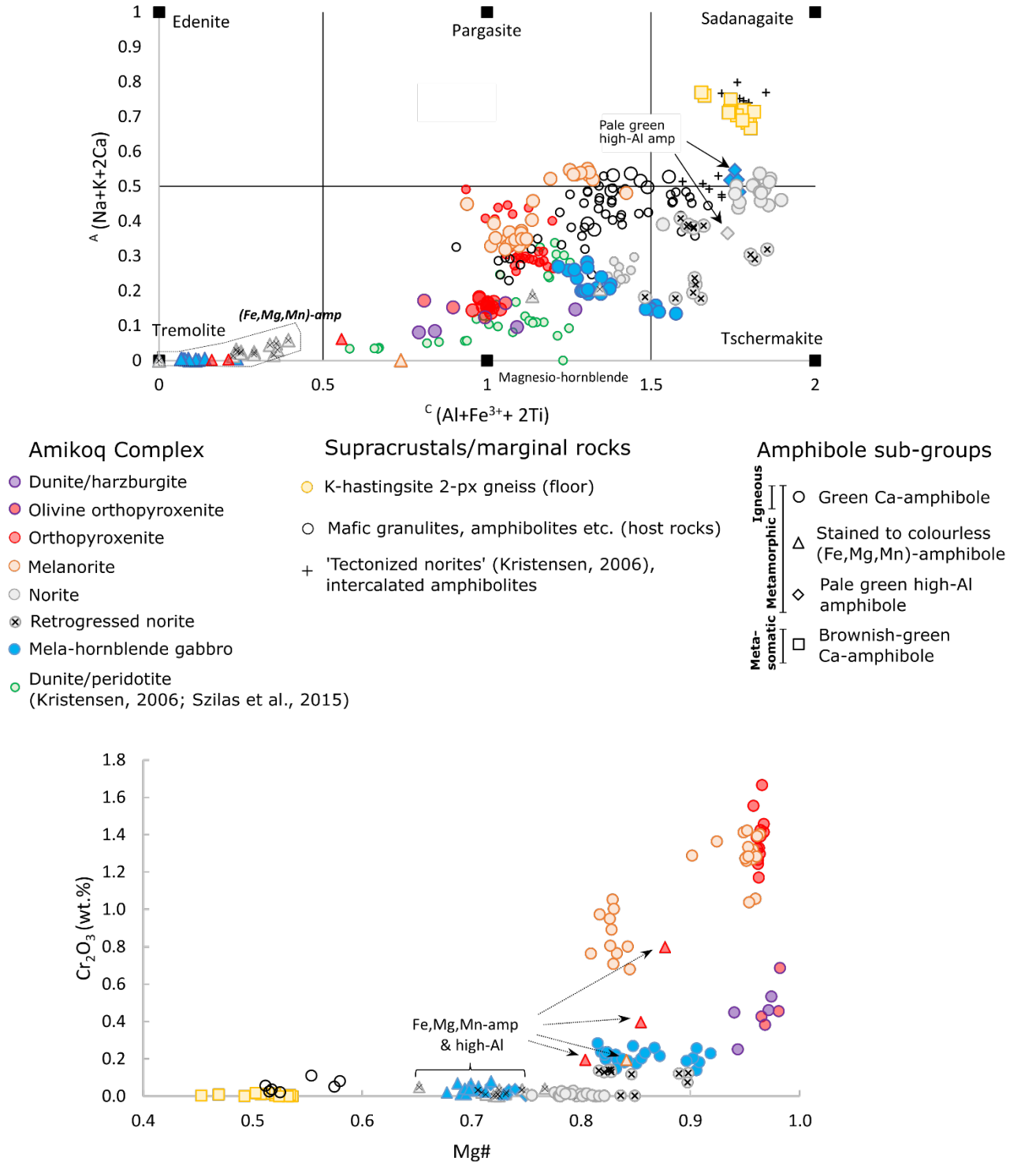

Fig. S16. a) Amphibole ^{A}(Na+K+2Ca) versus ^{C}(Al+Fe^{3+}+2Ti) classification diagram for Ca-amphiboles (Hawthorne et al., 2012). (Fe,Mg,Mn)-amp are also plotted for comparison though this diagram is inadequate in discriminating between different (Fe,Mg,Mn)-amp species. **b)** Amphibole Cr_2O_3 (wt.%) vs. amphibole Mg#. Both orthopyroxenite and melanorites tend to have elevated Cr-content, which may be an inherited igneous signature. Mg# = Mg / (Mg+Fe^{2+}).

Fig. S17. Garnet Profiles

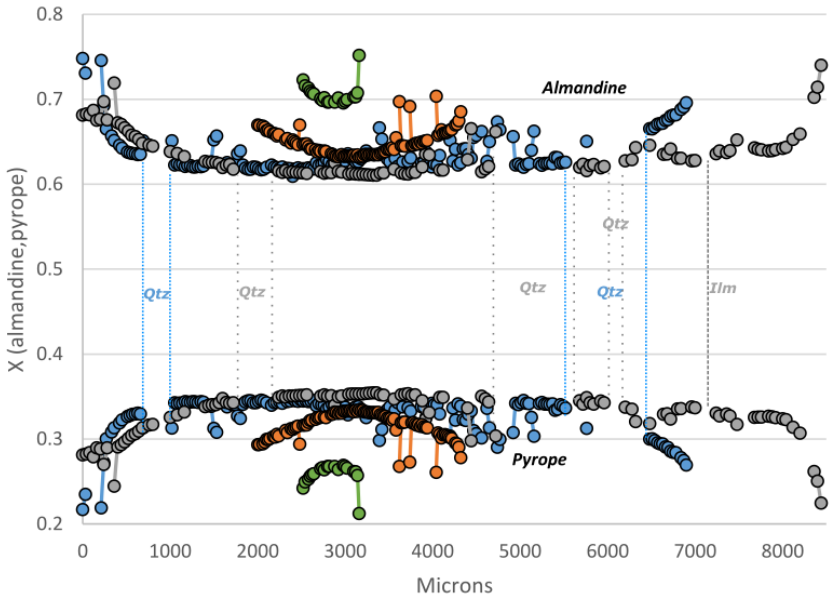

Fig. S17. Garnet rim-to-rim traverses. Almandine and pyrope components plotted against distance (microns). Colours correspond to individual garnet grains; the small garnet (green) does not record the high P-T recorded in cores of larger garnet (blue and grey). Quartz inclusions are indicated (see also Fig. A3g-h) as well as one small ilmenite (grey garnet); other gaps in the profiles correspond to discarded data points (see methods section).

Fig. S18 Additional amp geochem (Si vs. Mg#, $^{C}Fe^{3+}$ vs. Si) (500 dpi)

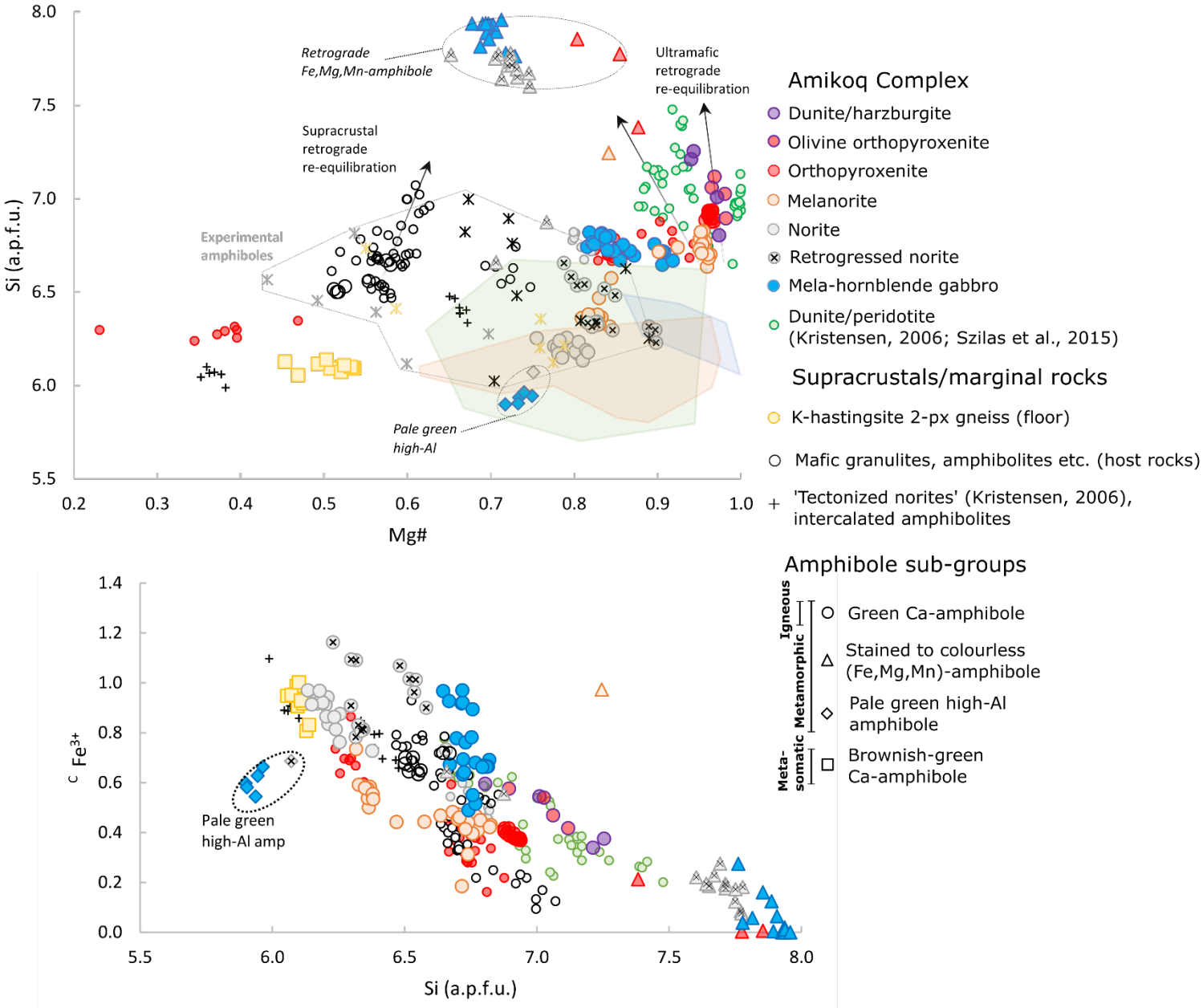

Fig. S18. a) Si (a.p.f.u.) versus Mg#. **b)** $^{C}Fe^{3+}$ versus Si (a.p.f.u.). Low Si appear to be coupled to high Fe^{3+} content – higher Fe^{3+} in retrogressed norites is probably owed to abundant magnetite, whereas the unretrogressed norite may have inherited the high Fe^{3+} content from a putative melt. See text for details. "Alaskan Complexes"-amphiboles are from Himmelberg & Loney (1995), "Arc xenolith"-amphiboles are from Arculus & Wills (1980), DeBari & Coleman (1989), DeBari et al. (1987) and Tollan et al. (2012), "Stillwater ultramafic"-amphiboles are from Page & Zientek (1987); average metamorphic amphibole (black diamond) composition from Schumacher (2007); experimental amphiboles are from Helz (1973, 1979); small symbols are Amikoq amphiboles from Kristensen (2006) and Szilas et al. (2015). All amphiboles have been recalculated using the spreadsheet of Locock (2014). Mg# = Mg / ($Mg+Fe^{2+}$).

Fig. S19. Temperature versus ^{T}Al-^{A}Na-^{A}K in amphibole. (500 dpi)

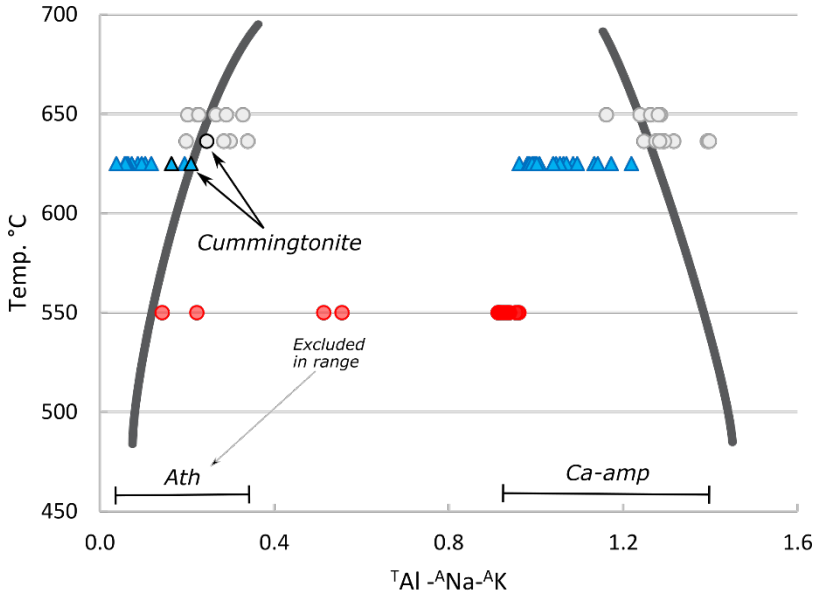

Fig. S19. Temperature versus ^{T}Al-^{A}Na-^{A}K in amphibole. Bars labelled "Ath" and "Ca-amp" denote the anthophyllite and Ca-amp range, respectively. The compositional range is considerably smaller for ^{B}(Na+Ca) (Fig. 12) than ^{T}Al-^{A}Na-^{A}K, which may indicate that the former is the more reliable parameter; especially the norites seem to indicate a relatively narrow T-range of ~500-650°C. Symbols with black rims are cummingtonites, otherwise as in Fig. S18 – note that the plotted norites are retrogressed varieties.